

Absolute coverage determination in the K/Si(111):B- $2\sqrt{3} \times 2\sqrt{3}R30^\circ$ surfaceC. Tournier-Colletta,^{1,*} L. Cardenas,¹ Y. Fagot-Revurat,¹ A. Tejada,^{1,2} B. Kierren,¹ and D. Malterre¹¹*Institut Jean Lamour, UMR 7198, Nancy Université/CNRS, B.P. 239 FE-54506, Vandoeuvre-lès-Nancy, France*²*Synchrotron Soleil, Cassiopée Beamline, B.P. 48 FE-91192, Gif-Sur-Yvette, France*

(Received 1 June 2011; revised manuscript received 23 September 2011; published 28 October 2011)

In this paper, we report on the experimental determination of alkali absolute coverage in the K/Si(111):B- $2\sqrt{3} \times 2\sqrt{3}R30^\circ$ surface. To this end, we carried out a comparative study with the closest system, namely, K/Si(111)- 3×1 , for which potassium coverage has been widely demonstrated to be $1/3$ of a monolayer. We used x-ray photoemission spectroscopy to count and compare the number of potassium atoms in both surfaces, together with a scanning tunneling microscopy in order to check the completion of these ultrathin layers. The analysis leads to a $1/2$ monolayer coverage in the $2\sqrt{3} \times 2\sqrt{3}R30^\circ$ surface, that is six potassium atoms per unit cell. Assuming this coverage, we can propose a simple model structure with potassium atoms arranged in trimers; we discuss the effect of such a reconstruction in terms of two distinct “up” and “down” Si adatom sites as well as the resulting surface electronic properties.

DOI: 10.1103/PhysRevB.84.155443

PACS number(s): 68.35.bg, 68.37.Ef

I. INTRODUCTION

Surfaces of bulk semiconductors are commonly subject to reconstructions upon deposition of metallic atoms. Perhaps the most famous example comes from the (111) face of silicon, whose clean surface itself adopts the rather complex 7×7 stable reconstruction. The so-called “dimer-adatom-stacking fault” (DAS) structural model^{1,2} proposed for this surface was nicely demonstrated by scanning tunneling microscopy (STM), and represented the first success of the emerging local probe. Concerning the electronic structure, the important point is the partial filling of the surface state associated with adatoms’ sp_z dangling bonds, making this surface metallic.^{3,4} Upon deposition of monovalent adsorbates (alkali and Ag atoms), for instance, the 7×7 reconstruction is destroyed at the benefit of the three-domain, one-dimensional 3×1 reconstruction.⁵⁻⁹ Basically, such a reconstruction is triggered because electrons provided by the adsorbates can, in addition to dangling electrons of the clean surface, lead to completely filled bands, which lower the electronic energy. The widely accepted atomic structure relies on the honeycomb chain-channel (HCC) model,¹¹ in which each unit cell contains one alkali atom, so that the coverage is $1/3$ of a monolayer (ML) with respect to the 1×1 undistorted unit cell. It is worth noting that, in the case of potassium (K) adsorbates, it has been possible to confirm the coverage experimentally using ion-scattering spectroscopy¹⁰ and x-ray photoemission spectroscopy (XPS).¹² In this structure, four surface states are predicted, three of which are filled in relative agreement with angle-resolved photoemission spectroscopy (ARPES) measurements.¹² In the case of divalent adsorbates (alkaline-earth and rare-earth metals), five reconstructions, starting from the 3×2 at $1/6$ monolayer (ML) and culminating in the 2×1 at $1/2$ ML, are observed;¹³ then surface atomic structure can change with small coverage differences only.

As already mentioned, the knowledge of the absolute coverage is also fundamental to understand the surface electronic structure, since it allows one to infer the number of unpaired surface electrons, and hence, the metallic or insulating nature of the surface states. Given that each of these can accommodate two electrons, an even (odd) number of

electrons should lead to completely (partially) filled bands, and then an insulating (metallic) surface. This is a simple electron counting rule, which holds true in a one-electron picture. However, metallic surface states on bulk semiconductors can exhibit important correlation effects, especially on the $\sqrt{3} \times \sqrt{3}R30^\circ$ (“ $\sqrt{3}$ ” hereafter)—reconstructed (111) surfaces, whose bandwidth is predicted to be small compared to the Coulomb repulsion energy U .^{14,17} Then electrons may be prevented from hopping and forming bands, resulting in the so-called Mott ground state with electron localization and antiferromagnetic ordering.^{15,16} The (inverse) photoemission signature of this broken-symmetry phase is similar to that of a band insulator: no weight at the Fermi energy but two weakly-dispersive Hubbard bands from both sides of E_F are observed, the gap in between being given by U . Here again, the knowledge of the number of electrons per unit cell is of the first importance, in order to distinguish between the Mott ground state and a mere band insulator scenario with correlation effects ruled out. Typical examples of partially filled surface states showing an insulating spectral signature are found on the $1/3$ ML Sn/Ge(111) and $1/3$ ML Si/SiC(0001) surfaces. In these systems, photoemission,^{18,19} inverse photoemission,²⁰ and scanning tunneling spectroscopy (STS)²¹ have evidenced almost flat, gapped surface states. Since *ab initio* (LDA) calculations predict metallicity, the Mott ground state has been invoked.^{18,22-24}

An older but less studied system is K/Si(111):B- $\sqrt{3}$. Two weakly-dispersive surface states with a large gap (≈ 1.5 eV) have been observed.²⁵⁻²⁷ Weitering *et al.* proposed that it could also be the signature of a Mott insulator,²⁷ since they assumed a coverage of one K atom per $\sqrt{3}$ unit cell ($1/3$ ML), which should lead to one half filled, metallic surface state in a one-electron picture.^{28,29} Very recently, the $2\sqrt{3} \times 2\sqrt{3}R30^\circ$ reconstruction (“ $2\sqrt{3}$ ” hereafter) together with a similar surface electronic structure as in Ref. 27 have been observed³⁰ and generalized to all alkali adsorbates,³¹ Still assuming a $1/3$ ML coverage would now give an even number of electrons (four) per $2\sqrt{3}$ unit cell and, therefore, produce a mere band insulator in contradiction with the former scenario. It is then very necessary to determine experimentally the absolute

coverage of the $2\sqrt{3}$ surface to solve the controversy, even it is not so easy from a practical point of view. In order to do that, we have carried out a comparative study with K/Si(111)- 3×1 , by combining low-energy electron diffraction (LEED), STM, and XPS. XPS is used first to check that K coverage does saturate; then as the 3×1 coverage is known, direct comparison of K-core level spectra would give the $2\sqrt{3}$ coverage. STM is used to check the completion of the ultrathin layers measured with XPS. Ultimately knowing the exact number of potassium atoms, it will be possible to propose a model structure for the $2\sqrt{3}$ surface and discuss its electronic properties.

II. EXPERIMENTAL DETAILS

Measurements have been performed in a ultrahigh vacuum setup, which couples a preparation chamber equipped with LEED and Auger spectroscopy, a photoemission chamber and a low-temperature STM (Omicron).

The substrate is a highly boron-enriched Si(111) sample ($\rho \approx 10^{-3} \Omega \text{cm}$). After a long outgassing, the sample is progressively flashed up to 1500 K. During this step, pressure never exceeds 2×10^{-9} mbar. Then follows a few-hour annealing at 1100 K, which makes boron atoms segregate to the surface. The $\sqrt{3} \times \sqrt{3} R30^\circ$ symmetry and long-range order are checked by LEED. The 7×7 surface is obtained from a standard *n*-doped Si(111) sample, which is flashed the same way as Si:B but annealed at 1100 K for a few minutes only. STM scans show clean surfaces nearly free of defects (especially boron vacancies in the case of Si:B). Potassium atoms are provided by commercial SAES getters; these are based on the thermally activated reduction of an alkali chromate. The getters have been carefully outgassed so that the pressure never exceeds 1×10^{-9} mbar (H_2 mainly) during evaporation. The evaporation procedure is always the same; we raise the current passing through the alkali getter up to 5 A by 1 A/min steps, once this operating current is reached, we wait 5 min before exposing the substrate in order to stabilize the alkali flux. To obtain the $2\sqrt{3}$ reconstruction, the Si:B- $\sqrt{3}$ surface is held at room temperature, whereas the 3×1 is produced by holding the Si- 7×7 surface at 700 K during evaporation. In the following, we would study these interfaces for increasing K coverages; in order to do that, we do not evaporate additional atoms on a same primary deposition but prepare a new clean surface for each desired coverage. Immediately after deposition, Auger spectroscopy (AES) characterization shows no significant O or C contamination, which can be a problematic issue when dealing with alkali films.⁴⁰

Photoemission measurements are carried out with a Scienta SES-200 hemispherical analyzer. The x-ray source works with the Mg $K\alpha$ radiation ($h\nu = 1253.6$ eV); since it is not monochromatized, the source resolution is about 0.8 eV only. For all spectra presented in this paper, we use constant working parameters for the source (emission current of 20 mA and high-voltage of 15 kV). In addition, photoemission data acquisition is done according to the following procedure: measurement at room temperature under a pressure of $1-2 \times 10^{-9}$ mbar, largest slit width (4.0 mm) in order to have significant signal/noise ratio on K core levels, 50-eV-pass energy, and a single sweep

per distinct core level. Finally, the sample position with respect to the x-ray tube is always the same. In the end, a very good reproducibility of photon flux and recorded core-level intensities is observed: the variation between two sample preparations and measurements is typically less than 10%. STM topographs of the 3×1 have been recorded at room temperature using a manually cut Pt-Ir tip, while the $2\sqrt{3}$ has been observed at liquid nitrogen temperature (77 K). The tip is prepared on the Au(111) surface in order to tailor its density of states, until the Shockley surface state is recovered in spectroscopic measurements.

III. COMPARATIVE LEED/XPS/STM STUDY OF TWO DISTINCT K/SI(111) SURFACES

A. K/SI(111)- 3×1

Let us begin with the reference system, namely K/Si(111)- 3×1 for which we have first correlated LEED and XPS measurements (see Fig. 1). Starting from the clean 7×7 surface (left LEED pattern on which the 1×1 first-order diffraction spots are indicated for clarity), K deposition leads to additional spots indicated by the white arrows (10 min evaporation, center pattern). To be more specific, we observe two new spots between zero-order and 1×1 first-order spots; they separate the 1×1 reciprocal lattice constant into three equal parts then they correspond to the expected 3×1 reconstruction. In addition, these spots appear in the three high-symmetry directions rotated by 120° , confirming the three-domain nature of the surface (the possibility of a single-domain 3×3 surface instead is ruled out as shown in STM topographs, Fig. 2). Up to 10 min evaporation, the 7×7 and the three 3×1 domains coexist at the surface with gradual increase of the 3×1 spots intensity. For higher deposition times (we performed 15 and 25 min evaporations, right LEED pattern being for the latter), the 7×7 domain has disappeared completely and a sharp 3×1 pattern is observed.

With LEED only, it is not possible to state *a priori* whether there is only one 3×1 -reconstructed layer or many of them stacked. However, the latter seems not realistic because this reconstruction does require Si atoms and the associated dangling electrons to be stabilized, so that it is not likely for an overlayer made of K atoms only to adopt this reconstruction. What is not excluded is that additional K atoms could form amorphous three-dimensional islands not detected by LEED; this hypothesis, again, will be ruled out by STM (see Fig. 2). We have performed XPS measurements on these samples in order to count K atoms, and we show that the number of K atoms saturates at this surface just after the first layer completion. We have focused on the K $2p$ core level because it gives the highest cross section at the employed photon energy (1253.6 eV). At the bottom of Fig. 1, we have plotted photoemission spectra as a function of electron kinetic energy, corresponding to different evaporation times. A weak (Shirley) background has been subtracted from the experimental data; this background has been determined simultaneously with the contribution of primary photoemitted electrons (plain lines, sum of two Lorentzian functions corresponding to the spin-orbit split $2p_{1/2}$ and $2p_{3/2}$ atomic configurations) by fitting experimental data. As expected, the K $2p$ line becomes more

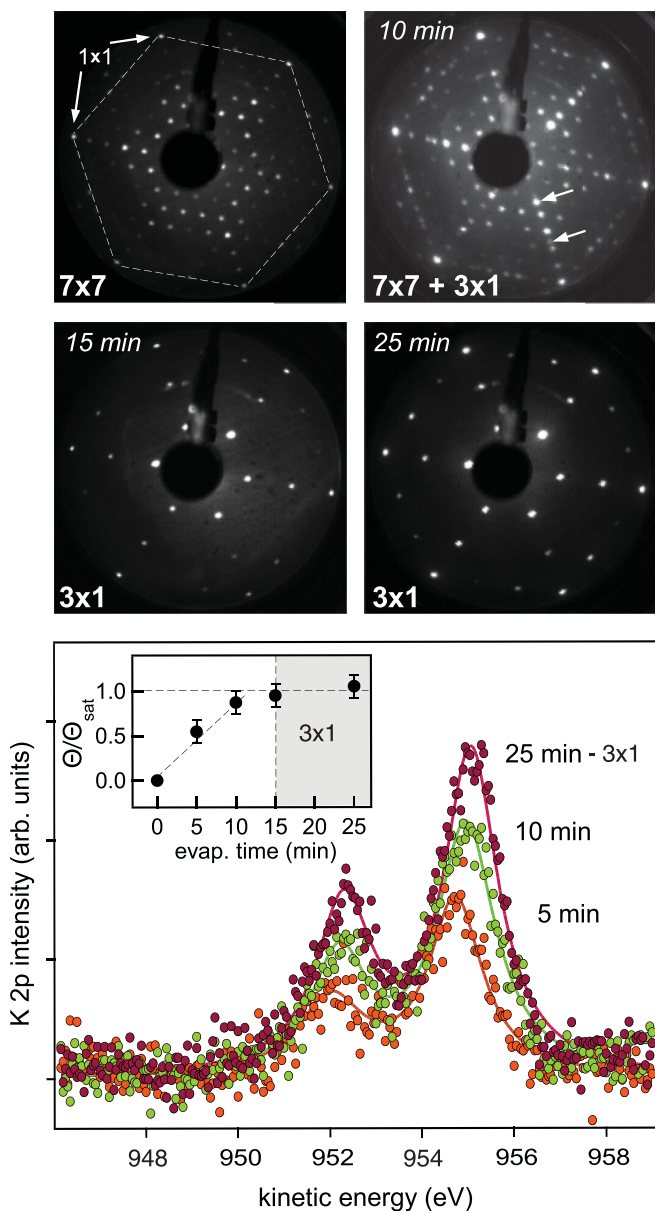


FIG. 1. (Color online) LEED-XPS study of K/Si(111)- 3×1 . Top: the LEED patterns show a coexistence of the three 3×1 domains—typical spots of one of them are indicated by white arrows—together with the substrate 7×7 surface; the latter disappears at the highest deposition times (electron primary energy $E = 30$ eV). Bottom: K $2p$ spectra corresponding to above LEED patterns, with the plain lines being simple fits; the inset shows the K coverage θ as a function of deposition time, obtained from the integrated area of the fits. θ clearly saturates once the 3×1 is the only observed reconstruction.

intense as the deposition time increases. From the integrated area of the fitted spin-orbit doublet, we deduce a quantity that is proportional to the number of K atoms or coverage θ . The inset shows clearly that θ saturates once the first 3×1 layer is completed, for 15 min evaporation, that is when the 7×7 spots disappear completely on LEED patterns. We have shown here data for the largest evaporation time (25 min), but they are mainly the same as for the 15 min, critical time.

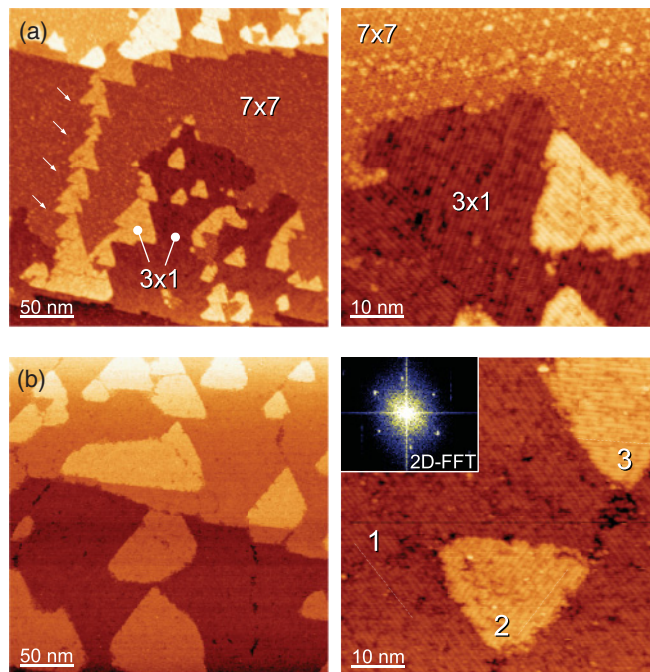


FIG. 2. (Color online) STM topographs of K/Si(111)- 3×1 (300 K). (a) Partial coverage. The large view (300×300 nm²; $U = -2.5$ V, $I = 0.2$ nA) shows the growth 3×1 phase on the 7×7 terraces, in a form of terraces at step edges (darkest areas) and triangular islands along the 7×7 domain boundaries (brightest areas, indicated by the white arrows); see Ref. 9 for a comprehensive study of the growth mechanism. The closest view (60×60 nm², same tunneling parameters) shows the boundary between the 7×7 and these two kinds of 3×1 domains. (b) Saturation coverage (25 min). On the large view ($U = -1.6$ V, $I = 0.5$ nA), terraces are shown to be completely covered by the 3×1 terraces and islands, which occupy similar areas. The closest view shows three 3×1 domains (1, 2, and 3) rotated by 120° , which give rise to a hexagonal Fourier transform (inset) in agreement with the LEED pattern (see Fig. 1).

Let us now discuss the real-space structure of the 3×1 surface, thanks to STM topographs (see Fig. 2). A comprehensive study of growth mechanisms has been carried out by Saranin *et al.*⁹ in the case of Na/Si(111)- 3×1 . We report here similar observations concerning K which, to the best of our knowledge, have not been documented in the literature. Thus we assume that K and Na growth modes are essentially the same. In Fig. 2 (a), we consider a partial coverage situation where 3×1 and 7×7 reconstructions coexist and give a LEED pattern similar to that presented in Fig. 1. On the large scale topograph (300×300 nm²; $U = -2.5$ V, $I = 0.2$ nA), we first distinguish the wide terraces of the Si(111) surface. In the central terrace, the 7×7 is observed far away from the descendant step (bottom of the topograph); however at this precise location, we observe a sawtooth step and from it, the development of a distinct 3×1 terrace, which appears darker than the 7×7 domain and penetrates into the Si(111) terrace. In addition to the 3×1 terraces, one observes the formation of triangular 3×1 islands, which nucleate on the 7×7 antiphase domain boundaries (indicated by the white arrows). These islands appear brighter than the 7×7 domain; this is not due to a second K layer stacked but

to a complex Si mass redistribution during the destruction of the 7×7 DAS structure.⁹ Ultimately, on both 3×1 terraces and islands, the K coverage has the same $1/3$ ML value. The closest view (60×60 nm², same tunneling parameters), shows the boundary between 7×7 and 3×3 (terrace and islands) domains. In fact, K clusters are observed on the 7×7 domain, so that it is more correct to view this domain as a mixture of native 7×7 and the so-called $\delta 7 \times 7$ cells.³² On the 3×1 terrace (dark), we distinguish two domains rotated by 120° , one of which has same orientation than the 3×1 island (bright). For the 25 min evaporation, that is saturation coverage according to our XPS calibration (see Fig. 1), we observe the (b) topographs. The “ 7×7 ” domain has disappeared in agreement with the LEED pattern. Si steps are now covered completely by 3×1 terraces and islands, both occupying similar areas. On the small scale image, we can identify three domains—two of which are islands—corresponding to the three high-symmetry directions indicated by the dotted lines. By making a two-dimensional fast Fourier transform (2D-FFT, see the inset), we lose the one-dimensional nature of the reconstruction and recover a hexagonal reciprocal lattice as in the LEED patterns.

B. K/Si(111): $B-2\sqrt{3}$

Now that we have characterized the saturated K/Si(111)- 3×1 reference surface, let us study the system, which interests us more, namely, K/Si(111): $B-2\sqrt{3}$, and determine its absolute coverage. In a similar way, we have first correlated LEED and XPS measurements (see Fig. 3). The left LEED pattern is for the clean Si(111): $B-\sqrt{3}$ surface; for clarity, we have indicated on it the 1×1 and $\sqrt{3}$ first-order spots by white dotted and plain yellow lines, respectively. In the low-coverage regime, that is for deposition times up to 70 s, no structural changes are observed with LEED, the $\sqrt{3}$ being preserved. Further deposition (90 s) leads to faint “ 3×3 ” spots indicated by the white arrows (center pattern), in addition to the $\sqrt{3}$ spots as already documented in Ref. 31. We use quotes in designating the reconstruction because we cannot exclude the superposition of three 3×1 domains as in the previous surface; furthermore, we have no STM images of the structure to confirm this point. Then, the “ 3×3 ” reconstruction is destroyed for a slightly longer deposition time, at the benefit of the $2\sqrt{3}$ one (105 s, right pattern). This structure is conserved for a significantly longer deposition time (180 s in this data set), suggesting alkali dosage saturation. We want to stress a special feature of this $2\sqrt{3}$ reconstruction concerning its growth mode: contrary to the 3×1 , there is no indication of small $2\sqrt{3}$ domains nucleation, the latter becoming larger as evaporation time increases (with increasingly intense diffraction spots), but rather a “spontaneous” ordering when saturation coverage is reached.

As for the 3×1 surface, saturation of alkali coverage is confirmed by analyzing K $2p$ spectra (bottom of Fig. 3). The coverage θ is obtained in a similar way as in Sec. III A. The inset shows clearly that θ saturates once the $2\sqrt{3}$ structure appears for 105-s evaporation. In Fig. 4, we present STM topographs recorded on a $2\sqrt{3}$ surface at 77 K. In Fig. 4(a), the long-range order of this single-domain hexagonal reconstruction is demonstrated on a 60×60 nm² area

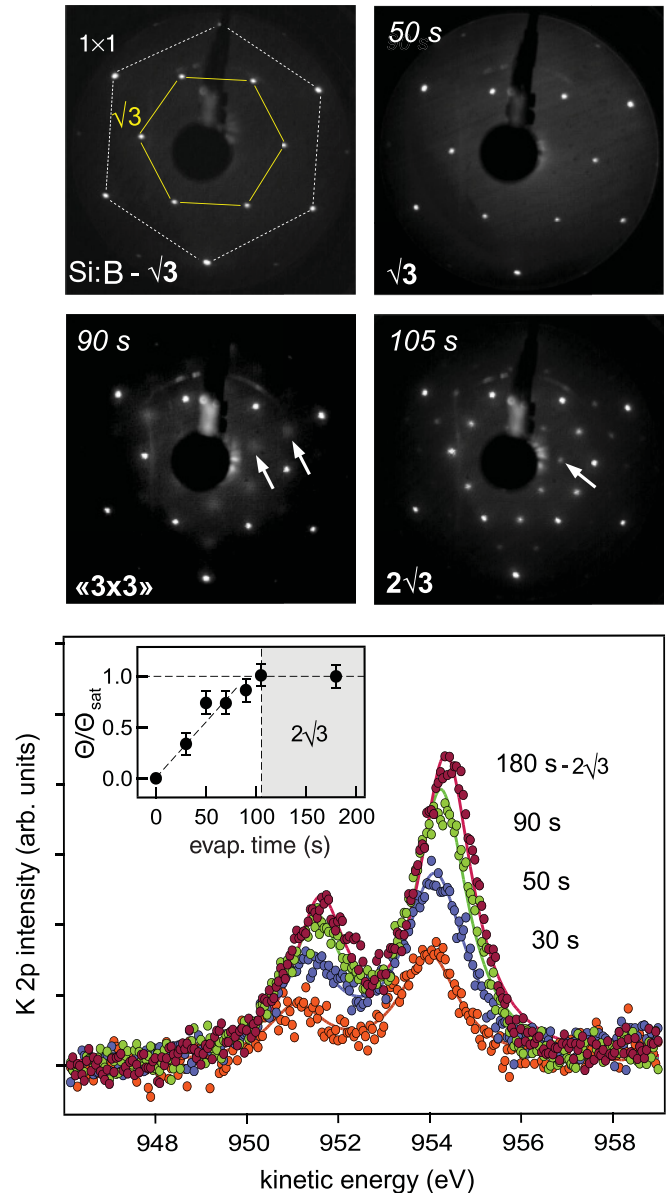


FIG. 3. (Color online) LEED-XPS study of K/Si(111): $B-2\sqrt{3}$. Top: the LEED patterns do not show any specific reconstruction until 90 s deposition time (center pattern) when faint 3×3 spots indicated by the white arrows are observed. Slightly longer time (105 s, right panel) destroys this structure at the benefit of the $2\sqrt{3}$, the latter being preserved for subsequent deposition (electron primary energy $E = 40$ eV). Bottom: K $2p$ spectra corresponding to above LEED patterns, with the plain lines being simple fits; the inset shows the K coverage θ as a function of deposition time, obtained from the integrated area of the fits. θ clearly saturates as soon as the $2\sqrt{3}$ is observed.

($U = +1.2$ V, $I = 0.1$ nA); the 2D-FFT reveals indeed relatively well defined spots showing hexagonal symmetry in agreement with LEED. By taking a closer view (b), we can identify the $2\sqrt{3}$ unit cell and measure the corresponding lattice constant (≈ 13.5 Å, that is twice the $\sqrt{3}$ parameter.^{34,35}) In addition, the layer exhibits very bright localized spots; the latter are attributed to intrinsic Si:B defects, namely, boron vacancies, which spectral signature is very similar.³⁵ We

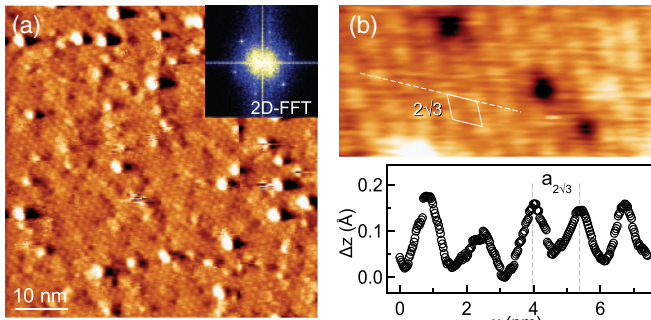


FIG. 4. (Color online) STM topographs of K/Si(111):B- $2\sqrt{3}$ (77 K). (a) $60 \times 60 \text{ nm}^2$ area showing $2\sqrt{3}$ long-range order, as demonstrated by the 2D-FFT in the inset ($U = +1.2 \text{ V}$, $I = 0.1 \text{ nA}$). (b) A closer view allows one to identify the $2\sqrt{3}$ unit cell and measure the expected lattice constant ($\approx 13.5 \text{ \AA}$).

found also dark spots maybe due to K vacancies. However, the concentration of such defects remains low so that the K coverage measured by XPS is essentially that of a perfect layer.

IV. ABSOLUTE COVERAGE DETERMINATION AND MODEL STRUCTURE FOR K/SI(111):B- $2\sqrt{3}$

Now that we have evidenced K saturation by XPS and checked the completion of a single layer by STM in both surfaces, it is possible to determine the absolute coverage of the K/Si(111):B- $2\sqrt{3}$. For that, we have plotted on Fig. 5(a) the raw K $2p$ spectra recorded on the 3×1 (purple balls) and $2\sqrt{3}$ (green balls) saturated samples, whose corresponding deposition times are 25 and 3 min, respectively. At first glance, the $2\sqrt{3}$ sample exhibits a signal that is significantly larger than on the 3×1 sample. By comparing directly the integrated area of the fits (plain lines, see Sec. III A for details), we find a ratio close to 3/2 between the $2\sqrt{3}$ and the 3×1 values. As we know saturation coverage to be 1/3 ML on the 3×1 surface,^{10,12} we deduce a coverage close to 1/2 ML on the $2\sqrt{3}$ surface. This value is very likely because it corresponds to six potassium atoms per $2\sqrt{3}$ unit cell, that is an integer number in agreement with an ordered structure. Upper (7 atoms, 0.58 ML) and lower (5 atoms, 0.42 ML) values are borderline if we consider a quite important $\pm 20\%$ error bar around 0.5 ML. The insert focuses on Si $2p$ spectra. The dashed lines stand for spectra recorded on pristine substrates, namely Si:B- $\sqrt{3}$ and Si- 7×7 . On saturated interfaces (balls), the Si $2p$ intensity is only slightly reduced due to diffusion by the K layer. It is about 90% of the substrate value in both cases. Moreover, raw Si $2p$ spectra recorded on the 3×1 and the $2\sqrt{3}$ samples have very similar intensities. This is an indirect confirmation of the nearly identical photon flux in both experiments, which validates *a posteriori* alkali coverage determination by direct comparison of K $2p$ spectra.

In Fig. 5(b), we propose a structural model for the $2\sqrt{3}$ surface assuming 6 K atoms per unit cell. The $2\sqrt{3}$ unit cell is indicated by the thick black line; it comprises four $\sqrt{3}$ unit cells, one being represented for clarity (dashed line). We first recall the basic atomic structure of the undistorted substrate surface:³⁴ the $\sqrt{3}$ lattice is formed by Si adatoms (one per unit cell) beneath which, in the third atomic layer, are located

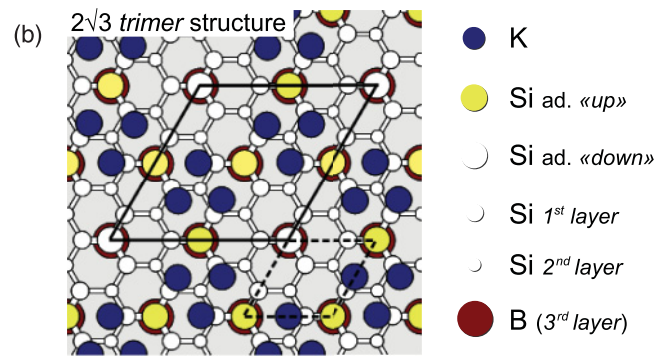
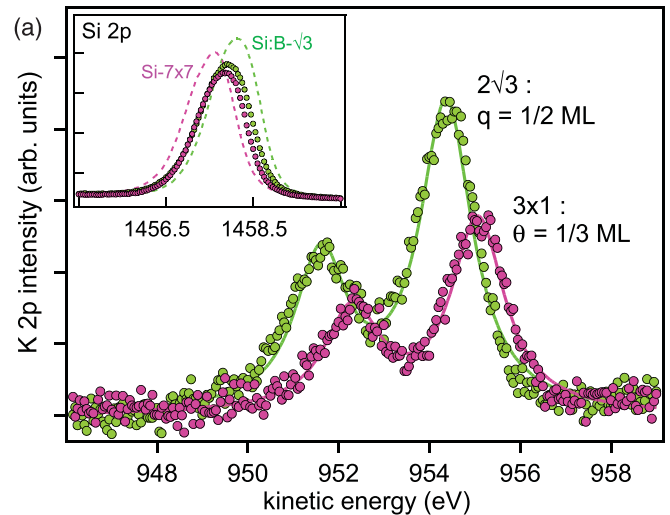


FIG. 5. (Color online) Absolute K coverage and model structure for K/Si(111):B- $2\sqrt{3}$. (a) Raw K $2p$ spectra recorded on $2\sqrt{3}$ (green balls) and 3×1 (purple balls, reference) saturated surfaces. The insert shows Si spectra, where balls and dashed lines stand for alkali-covered interfaces and Si substrates, respectively. Direct comparison of integrated areas gives a 0.5 ML ($\pm 10\%$) coverage for the $2\sqrt{3}$ surface (see text for a detailed discussion) (b) $2\sqrt{3}$ “trimer” structure, assuming six potassium atoms per unit cell in agreement with the coverage determined in (a).

those B atoms that have segregated during annealing. We have also represented Si atoms from the first and second subsurface layers because they are important in understanding possible adsorption sites. In the case of K adsorption, DFT calculations have evidenced the so-called H_3 site to be energetically favorable;²⁹ on this hollow adsorption site, each K atom (dark blue balls) forms three bonds, the first two with the nearest two Si adatoms and the third one with the Si atom from the first layer. Our preliminary energy-dependent LEED simulations seem to confirm this result. In addition, since a single adsorption site is found with XPS,³⁷ we assume the 6 K atoms to be located in this H_3 site. Then it is straightforward to propose an ordered $2\sqrt{3}$ pattern; indeed, by arranging K atoms in the form of two trimers, we get a highly symmetrical structure with all K atoms equivalent. Up to this point, the substrate structure has not been modified at all; this is consistent with the experimental finding that backbond states are not disrupted by K adsorption,²⁶ However, this cannot hold in the geometry we propose because we get two chemically inequivalent Si adatom sites, again in

agreement with XPS measurements;^{33,37} they are depicted by the white and yellow balls, which correspond to adatoms far and close to K trimers, respectively. Adatoms close to K atoms may experience a more important charge transfer from 4s electrons, and thus we expect these adatoms to buckle in order to screen the additional electronic charge.³⁹ Recent dual-bias STM imaging and high-resolution XPS measurements agree with the proposed atomic structure.³⁸

We finish by discussing the main consequences on surface electronic structure. On the Si:B substrate, each Si adatom provides an empty sp_z dangling orbital then the associated surface states appear in the unoccupied part of the spectrum.³⁴ Upon K deposition, these states are partially populated by electrons transferred from K 4s orbitals. According to DFT calculations,^{34,38} K atoms are completely ionized when deposited on the $\sqrt{3}$ substrate. Interestingly, this is not the case on alkali/Si(111)- 3×1 where alkali s orbitals contribute significantly to the occupied surface states.¹¹ This explains probably why the K 2*p* state appears at a higher kinetic energy (i.e., lower binding energy because of the larger valence electronic density screening the nucleus potential) in the 3×1 surface [see Fig. 5(a)]. Getting back to the $2\sqrt{3}$ structure, we get six electrons to be shared by the four Si dangling orbitals. Remember that three of them are near potassium trimers [yellow balls, which correspond to buckled Si adatoms, see Fig. 5(b)] so electrons would prefer to occupy these orbitals rather than the remaining isolated dangling orbital (white ball). In the end, the six electrons can fill completely the three surface states originating from the three equivalent buckled Si adatoms, while the state relative to the isolated adatom is left empty. This point is confirmed by recent DFT calculations.³⁸

Therefore the important point is that it is now possible to get an insulating surface electronic structure without invoking strong correlation effects. In this case, since the states are fully occupied, correlation effects cannot trigger an electronic instability like the Mott metal-to-insulator transition. We have recently evidenced with ARPES two of these occupied surface states using symmetry arguments; the third one is probably very difficult to deconvolve because of significant polaronic effects, which broaden the states on an energy scale larger than their bandwidth.³¹

V. CONCLUSION

By combining LEED, XPS, and STM, we have determined the absolute alkali coverage of K/Si(111):B- $2\sqrt{3}$ to be 1/2 ML, rather than 1/3 ML as assumed in the previous studies. This corresponds to six K atoms in the $2\sqrt{3}$ unit cell instead of four. This result has important consequences in understanding the surface electronic properties. Indeed, in that trimer structural model we have proposed and justified, we find that a 1/2 ML coverage leads to three fully occupied states and thus an insulating surface electronic structure. Then strong correlation effects are probably not the driving force of the insulating nature of this surface. Ultimately, relying on the trimer model, we have started DFT calculations³⁸ and it will be possible soon to compare band structure calculations to photoemission measurements.

ACKNOWLEDGMENTS

This work has received the financial support of the French ANR SURMOTT program (ANR-09-BLAN-0210-01).

*tournier@ijl.nancy-universite.fr

¹G. Binnig, H. Rohrer, Ch. Gerber, and E. Weibel, *Phys. Rev. Lett.* **50**, 120 (1983).

²K. Takayanagi, Y. Tanishiro, S. Takahashi, and M. Takahashi, *Surf. Sci.* **164**, 367 (1985).

³R. I. G. Uhrberg, T. Kaurila, and Y.-C. Chao, *Phys. Rev. B* **58**, R1730 (1998).

⁴I. Barke, F. Zheng, A. R. Konicek, R. C. Hatch, and F. J. Himpsel, *Phys. Rev. Lett.* **96**, 216801 (2006).

⁵W. C. Fan and A. Ignatiev, *Phys. Rev. B* **41**, 3592 (1990).

⁶T. Hashizume, Y. Hasegawa, I. Sumita, and T. Sakurai, *Surf. Sci.* **246**, 189 (1991).

⁷J. M. Carpinelli and H. H. Weitering, *Surf. Sci.* **331-333**, 1015 (1995).

⁸J. J. Paggel, G. Neuhold, H. Haak, and K. Horn, *Phys. Rev. B* **52**, 5813 (1995).

⁹A. A. Saranin, A. V. Zotov, S. V. Ryzhkov, D. A. Tsukanov, V. G. Lifshits, J.-T. Ryu, O. Kubo, H. Tani, T. Harada, M. Katayama, and K. Oura, *Phys. Rev. B* **58**, 7059 (1998).

¹⁰T. Hashizume, M. Katayama, D. Jeon, M. Aono, and T. Sakurai, *Jpn. J. Appl. Phys.* **32**, L1263 (1993).

¹¹S. C. Erwin and H. H. Weitering, *Phys. Rev. Lett.* **81**, 2296 (1998).

¹²K. Sakamoto, T. Okuda, H. Nishimoto, H. Daimon, S. Suga, T. Kinoshita, and A. Kakizaki, *Phys. Rev. B* **50**, 1725 (1994).

¹³C. Battaglia, P. Aebi, and S. C. Erwin, *Phys. Rev. B* **78**, 075409 (2008).

¹⁴E. Tosatti and P. W. Anderson, *J. Appl. Phys. Suppl.* **2**, Pt. 2 (1974).

¹⁵N. F. Mott, *Proc. R. Soc. A* **62**, 416 (1949).

¹⁶J. Hubbard, *Proc. R. Soc. A* **276**, 238 (1964); **277**, 237 (1964); **281**, 401 (1964).

¹⁷W. A. Harrison, *Phys. Rev. B* **31**, 2121 (1985).

¹⁸R. Cortes, A. Tejada, J. Lobo, C. Didiot, B. Kierren, D. Malterre, E. G. Michel, and A. Mascaraque, *Phys. Rev. Lett.* **96**, 126103 (2006).

¹⁹L. I. Johansson, F. Owman, and P. Martensson, *Surf. Sci.* **360**, L478 (1996).

²⁰J.-M. Themlin, I. Forbeaux, V. Langlais, H. Belkhir, and J.-M. Debever, *Europhys. Lett.* **39**, 61 (1997).

²¹V. Ramachandran and R. M. Feenstra, *Phys. Rev. Lett.* **82**, 1000 (1999).

²²G. Profeta and E. Tosatti, *Phys. Rev. Lett.* **98**, 086401 (2007).

²³G. Santoro, S. Scandolo, and E. Tosatti, *Phys. Rev. B* **59**, 1891 (1999).

²⁴J. E. Northrup and J. Neugebauer, *Phys. Rev. B* **57**, R4230 (1998).

²⁵T. M. Grehk, L. S. O. Johansson, U. O. Karlsson, and A. S. Flodström, *Phys. Rev. B* **47**, 13887 (1993).

²⁶H. H. Weitering, J. Chen, N. J. DiNardo, and E. W. Plummer, *Phys. Rev. B* **48**, 8119 (1993).

- ²⁷H. H. Weitering, X. Shi, P. D. Johnson, J. Chen, N. J. DiNardo, and K. Kempa, *Phys. Rev. Lett.* **78**, 1331 (1997).
- ²⁸C. S. Hellberg and S. C. Erwin, *Phys. Rev. Lett.* **83**, 1003 (1999).
- ²⁹H. Q. Shi, M. W. Radny, and P. V. Smith, *Phys. Rev. B* **70**, 235325 (2004).
- ³⁰L. A. Cardenas, Y. Fagot-Revurat, L. Moreau, B. Kierren, and D. Malterre, *Phys. Rev. Lett.* **103**, 046804 (2009).
- ³¹C. Tournier-Colletta, L. Cardenas, Y. Fagot-Revurat, B. Kierren, A. Tejada, D. Malterre, P. Le Fèvre, F. Bertran, and A. Taleb-Ibrahimi, *Phys. Rev. B* **82**, 165429 (2010).
- ³²H. Daimon and S. Ino, *Surf. Sci.* **164**, 320 (1985).
- ³³Y. Ma, J. E. Rowe, E. E. Chaban, C. T. Chen, R. L. Headrick, G. M. Meigs, S. Modesti, and F. Sette, *Phys. Rev. Lett.* **65**, 2173 (1990).
- ³⁴H. Q. Shi, M. W. Radny, and P. V. Smith, *Phys. Rev. B* **66**, 085329 (2002).
- ³⁵M. Berthe, A. Urbieto, L. Perdigao, B. Grandidier, D. Deresmes, C. Delerue, D. Stiévenard, R. Rurali, N. Lorente, L. Magaud, and P. Ordejon, *Phys. Rev. Lett.* **97**, 206801 (2006).
- ³⁶S. Hüfner, *Photoemission Spectroscopy: Principles and Application*, 3rd ed. (Springer, 2003).
- ³⁷C. Tournier-Colletta *et al.* (unpublished).
- ³⁸L. Chaput, C. Tournier-Colletta, L. A. Cardenas, Y. Fagot-Revurat, A. Tejada, B. Kierren, D. Malterre, P. Le Fèvre, F. Bertran, A. Taleb-Ibrahimi, D. G. Trabada, J. Ortega, and F. Flores,.
- ³⁹A. Zangwill, *Physics at Surfaces* (Cambridge University Press, 1988).
- ⁴⁰P. Soukiassian, J. A. Kubby, P. Mangat, Z. Hurych, and K. M. Schirm, *Phys. Rev. B* **46**, 13471 (1992).